Construction of Open-Source Laboratory-Scale Binder Jetting System for High-Speed Synchrotron X-Ray Imaging

Jacob Lawrence, Hector Andres Peña Vega, Bryant Stegman, Caleb Roberts, Joseph Spencer, Clinton James, McKay Christensen, Nathan Crane

Department of Mechanical Engineering, Brigham Young University, Provo, UT 84602

Abstract

Although commercial binder jetting (BJ) printers are available, they typically do not allow sufficient control over process parameters needed to study fundamental process characteristics. This work presents an overview of the design and construction of a custom BJ system used to observe fundamental phenomena in the BJ process. CAD models for the design and information on the software of this system is also given. This system will help elucidate the mechanisms that introduce part defects and other challenges unique to the BJ process. The BJ system was designed for both laboratory-scale experiments with a 100 x 100 mm build box and high-speed synchrotron X-ray imaging with a 500 μm thick powder bed, requiring high-accuracy motion stages and a controller with precise timing. The printer includes functionality for depositing and rolling powder, printing multi-layer parts, and direct observation of the jetting nozzle. This BJ system has enabled experiments that provide insight into the printing process that will aid future efforts to mitigate challenges associated with BJ.

Introduction

Binder Jetting (BJ) is an additive manufacturing (AM) process that has received added focus in recent years [1]. It utilizes an aqueous binder which is ink-jetted, layer by layer, onto a prepared powder bed to form geometry. This process involves powder deposition onto a powder bed, rolling powder to create a smooth surface, ink-jetting binder droplets in precise locations, and lowering the build space for the next layer. These steps repeated create a part that can then be removed from the loose powder and sintered to a final part [1, 2]. Control over each aspect of the operation gives opportunity for precise experiments to better understand BJ.

BJ along with other AM processes can manufacture parts with extreme complexity, can vary part shape without additional tooling, and builds parts directly from 3D models [3, 4]. BJ has distinct advantages relative to other AM methods including the separation of the formation step from the sintering process, allowing for greater microstructural control of the final piece [1]. BJ volume production can also be scaled with relative ease for either low or high-volume production of parts. This is accomplished by increasing the number of nozzles used and/or stacking many parts in one build volume. Additionally, BJ can print with nearly any powder feedstock. Testing has been done with copper, stainless steel, sand, and other ceramics [5-8], although metal powder is commonly used. These unique beneficial characteristics make BJ a highly attractive manufacturing process [1]. Although these capabilities are promising, the BJ process requires extensive study due to porosity defects that are introduced during the process as shown by previous research [6, 9]. Research shows that porosity defects in BJ parts form during the printing process by mechanisms such as powder bed flow and spreading, powder particle size, inkjet droplet impact onto the powder bed, and agglomerate formation of binder and powder [10-13]. With further study

of BJ process, these mechanisms can be more fully understood and printing parameters that minimize defect formation can be determined.

Commercial binder jetting machines such as the X1-Lab made by ExOne have been used to study the binder jetting process using high-speed X-ray imaging [14]. These and other commercial systems such as ExOne's R2 and Innovent systems have been used for other studies [5, 6, 13]. However, a custom system provides distinct advantages over existing commercial solutions including greater control over printer configuration, capabilities, and user-programmable printing parameters. Open-source binder jetting machines such as the Oasis 3DP and Plan B systems provide low-cost alternatives to commercial solutions but lack high-accuracy motion systems, fine control over printing parameters, hopper-fed powder deposition, and direct observation of printheads for measurement and maintenance.

Custom laboratory-scale BJ systems have been constructed for studying the BJ process [15, 16]. The system designed and constructed by Oropeza and Hart [16] includes micron accuracy motion, a heat lamp for curing deposited binder, a single piezoelectric nozzle for control of jetting parameters, a droplet observation system, and a powder bed equipped with a load cell for powder flow measurement and quantification. These capabilities enable numerous controlled experiments to better understand the BJ process [16]. However, the design has not been optimized for outside imaging. A printer with an exposed build box during printing is ideal for tests involving an outside source video capture of the process such as high-speed X-ray synchrotron imaging.

Outlined in this work is a design for a custom laboratory-scale BJ system [17] with optimization for X-ray imaging, ability to easily configure and program the printer for desired testing, micron accuracy motion, a single-nozzle printhead with control of jetting parameters, hopper-fed powder deposition, and a droplet observation system to quantify droplet features using a stroboscopic effect to capture droplet motion [18].

Design

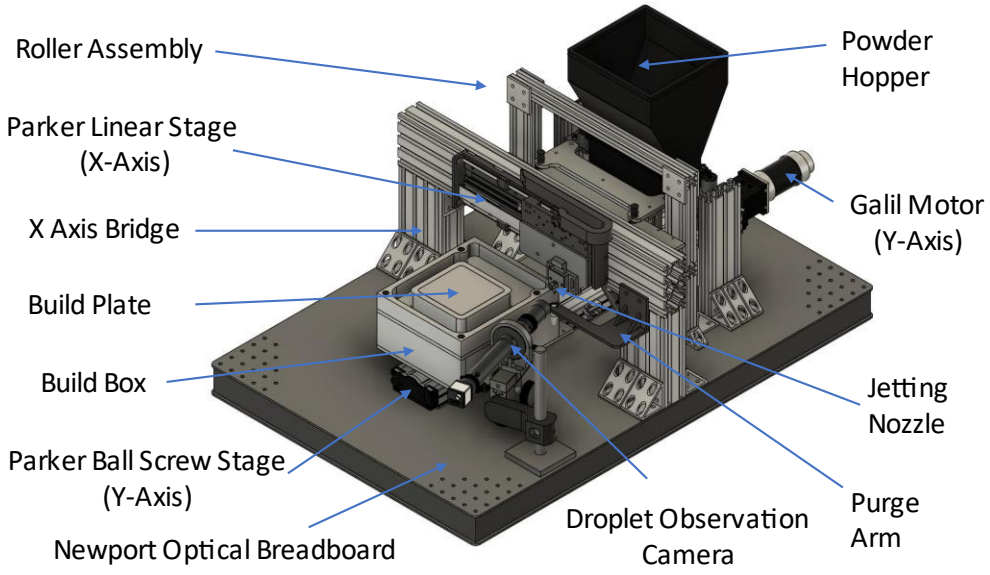

Figure 1. A CAD model [17] of the custom BJ printer with key components labeled.

System Overview

The printer is capable of automated powder deposition, powder spreading, and printing enabling multi-layer experiments to study the BJ process. As seen in Table 1, the printer uses a 100 mm square build plate with 15 mm of travel. The build box can be removed for part curing and extraction. The printer uses two motion stages to position the single nozzle printhead and a third motion stage to move the build platform for multi-layer printing. The printer is equipped with an integrated USB camera for observing and measuring jetting performance of the printhead. The printer is controlled with custom desktop software that runs on a host computer. More information on printer components is available in the following sections. A repository of CAD files for the printer can be found here [17].

Table 1. Key printer specifications of the custom BJ system.

Parameter	Value
Build Volume	100 x 100 x 15 mm (L x W x H)
Machine Dimensions	1040 x 600 x 474 mm (L x W x H)
Motor Step Size	1.0 x 1.25 x 0.5 µm (X, Y, Z)
Maximum Traverse Velocity	3000 x 300 x 5 mm/s (X, Y, Z)
Printhead	MicroFab Single-Nozzle Drop-on-Demand

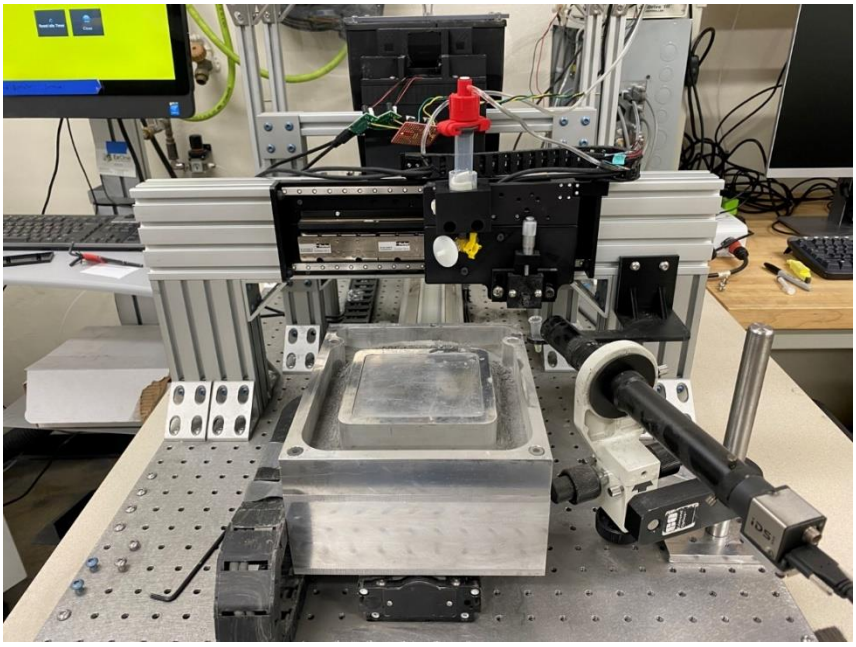

Figure 2. The custom BJ system configured with the full-sized build box for laboratory testing.

Linear Motion System

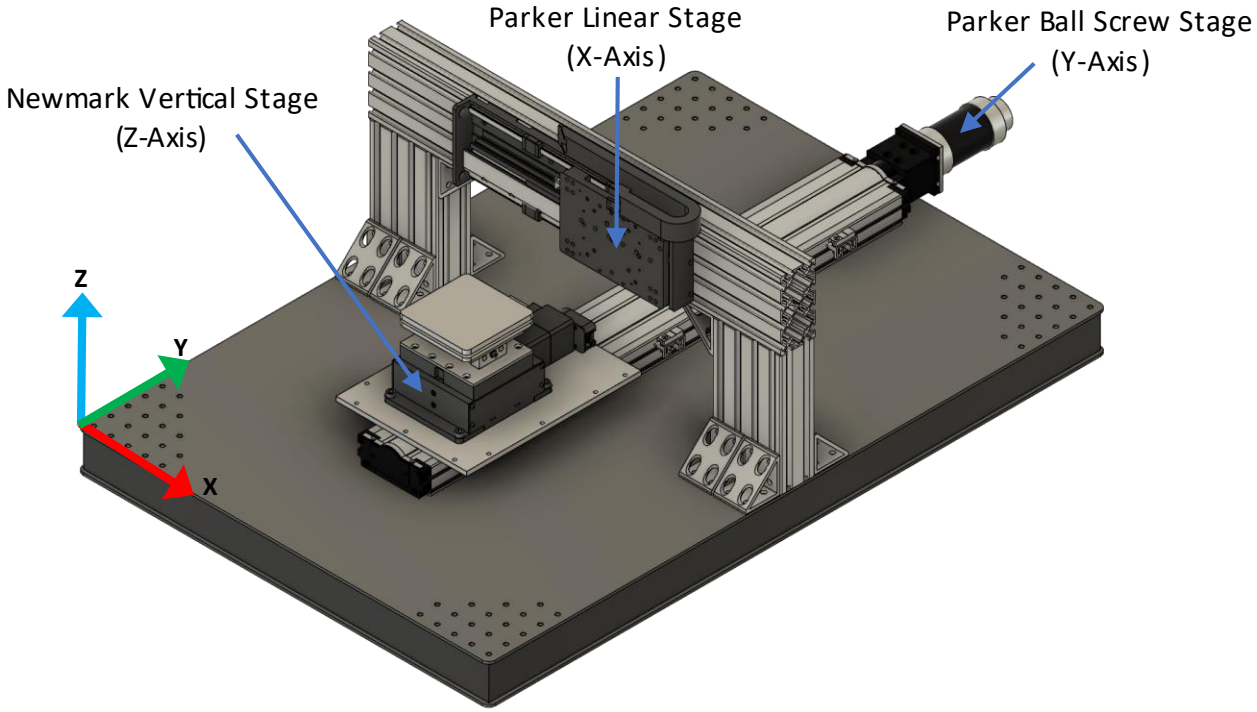

Figure 3. CAD model [17] of the linear motion system of the printer. It allows movement in all three axes X, Y, and Z.

The printer uses three motion stages for positioning the jetting nozzle, build box, and build platform. The X-axis positions the printhead and is mounted above the Y-axis on a bridge. The Y-axis moves the build box assembly and is mounted directly to the baseplate. The Z-axis actuates the build plate vertically and is mounted to the Y-axis.

X-Axis

The X-axis (Parker mSR100) is responsible for positioning the inkjet printhead in the primary jetting direction. The motion stage has 150 mm of travel and a maximum speed of 3000 mm/s. From manufacturer testing, the stage used has a measured accuracy of 3.3 µm and a bidirectional repeatability of 1.6 µm. The X-axis is also used to position the printhead to the rightmost limit of the stage for printhead maintenance and jetting observation.

Y-Axis

The Y-axis (Parker 404XR) is responsible for positioning the build box assembly for powder spreading, rolling, and printing. At 500mm in length, the Y-axis can move the build box along most of the length of the printer and is used for powder deposition, rolling, and printing. The manufacturer lists a positional accuracy of 34 µm and a bidirectional repeatability of 3.0 µm. The stage uses a Galil BLM-N23 servo motor with rotary encoder that results in a 1.25 µm encoder resolution along the length of the stage.

Z-Axis

The Z-axis (Newmark VS-15-2) is responsible for positioning the build plate and is used for moving the powder bed during multi-layer printing. The stage is mounted on the Y-axis and attaches to the build plate using a manual actuating gripper to allow for build box removal. More information is available in the section on the removable build box. The stage has 15 mm of travel, and the manufacturer lists an accuracy of 10 µm and a repeatability of 1 µm.

Motion Controller

The three motion stages are controlled by a Galil DMC-4080 motion controller with an AMP-D3547 amplifier module allowing for control of both brushless servos and stepper motors. The motion controller receives commands over ethernet from a host PC which are then processed to move the stages as desired. More information on the custom software used by the host PC to send commands to the motion controller is available in the control software section.

Inkjet Printhead

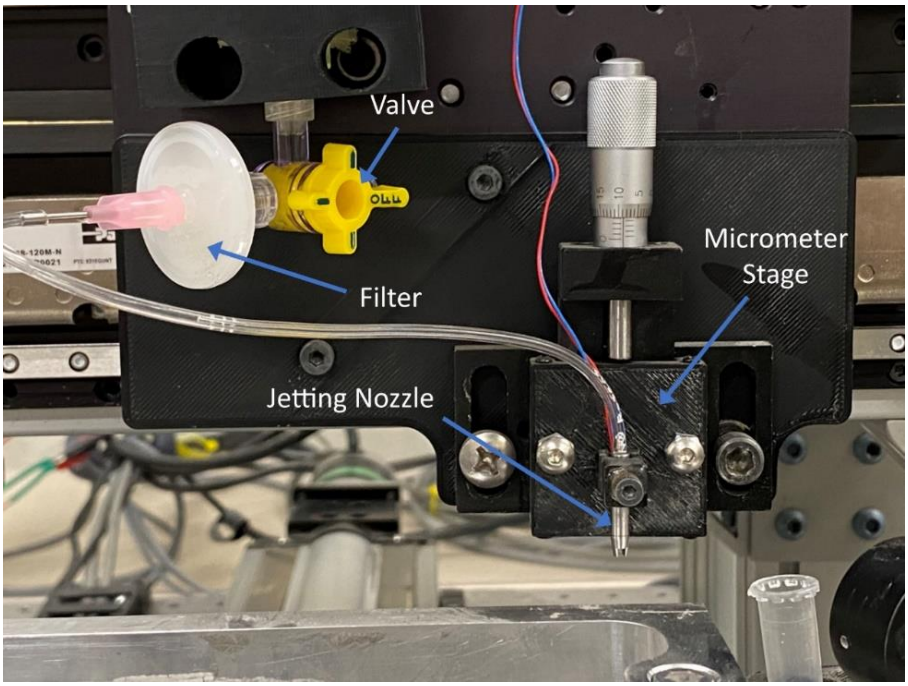

Figure 4. Inkjet printhead assembly. Binder used for printing is stored in a syringe which is mounted to the X-axis above the printhead. The jetting nozzle is mounted in an attachment on a micrometer stage to allow precise changes of the nozzle height along the Z-axis.

The printer uses a single nozzle drop-on-demand piezoelectric printhead (MicroFab MJ-AB) controlled by a JetDrive III controller. The printhead is mounted to a manual micrometer stage connected to the X-axis, allowing for positioning the nozzle at a desired height above the powder bed. Binder is stored in a syringe mounted to the X-axis. Backpressure in the binder supply is controlled with a MicroFab pneumatics console.

Droplet Observation

The droplet observation system (Figure 5) enables visual confirmation of stable jetting and estimation of droplet velocity. Observation is accomplished using a USB camera (IDS UI-3370CP-M-GL), a zoom lens (Edmund Optics VZM 450 Zoom Imaging Lens), and a strobing LED. The LED is connected to the JetDrive controller and synchronized with the jetting frequency to create a stroboscopic effect to enable visualization of droplets at much lower framerates than traditionally required.

Estimating Droplet Velocity

Droplet velocity is an important parameter when studying the BJ process. By gradually increasing temporal strobe offsets compared to jetting pulses, the droplet observation camera captures a video depicting a droplet as it exits the printhead nozzle (Figure 6). This video can be used to estimate the droplet velocity by comparing relative droplet positions between frames and calculating how fast it moves between each position. Droplet tracking and velocity estimation is done by a MATLAB script that analyzes the video. Jetting parameters can then be changed, and droplet velocity estimated again until the desired jetting velocity is reached.

Estimating Droplet Volume

Droplet volume is another important printing parameter in the BJ process. A volume measurement is conducted by first measuring the mass of a small plastic container. The printer then jets binder droplets at 1000 Hz for three minutes into the container. The container with binder is weighed again to obtain the total mass of droplets jetted during the three minutes. The binder volume is calculated from the measured binder density (1.05 g/cm^3). Then the total volume is divided by the number of droplets jetted during the three minutes to obtain an average volume of a single droplet. Average droplet diameter can also be estimated assuming a spherical droplet shape.

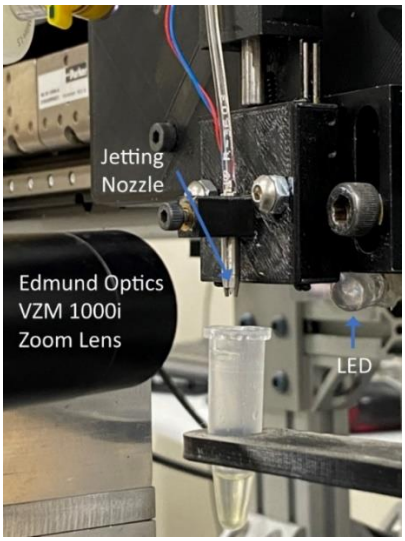

Figure 5. Droplet observation setup. The jetting nozzle is positioned between camera and a strobing LED for imaging and maintenance.

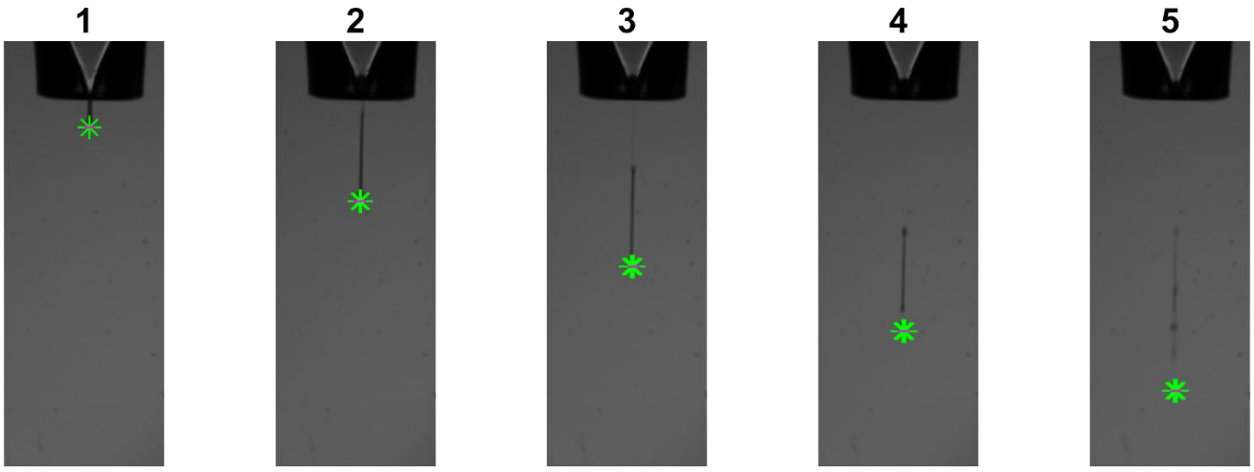

Figure 6. Sequence of binder droplets captured by the droplet observation camera. The velocity of the droplet can be calculated by tracking the droplet position between frames.

Powder Deposition and Spreading

The printer includes a powder hopper and roller for automated powder rolling and spreading. The hopper and the 12mm roller are components used in the ExOne Innovent+. The hopper is powered using a Telsonic SG4L Pro Screening Generator which is controlled via RS-232 from the Galil motion controller.

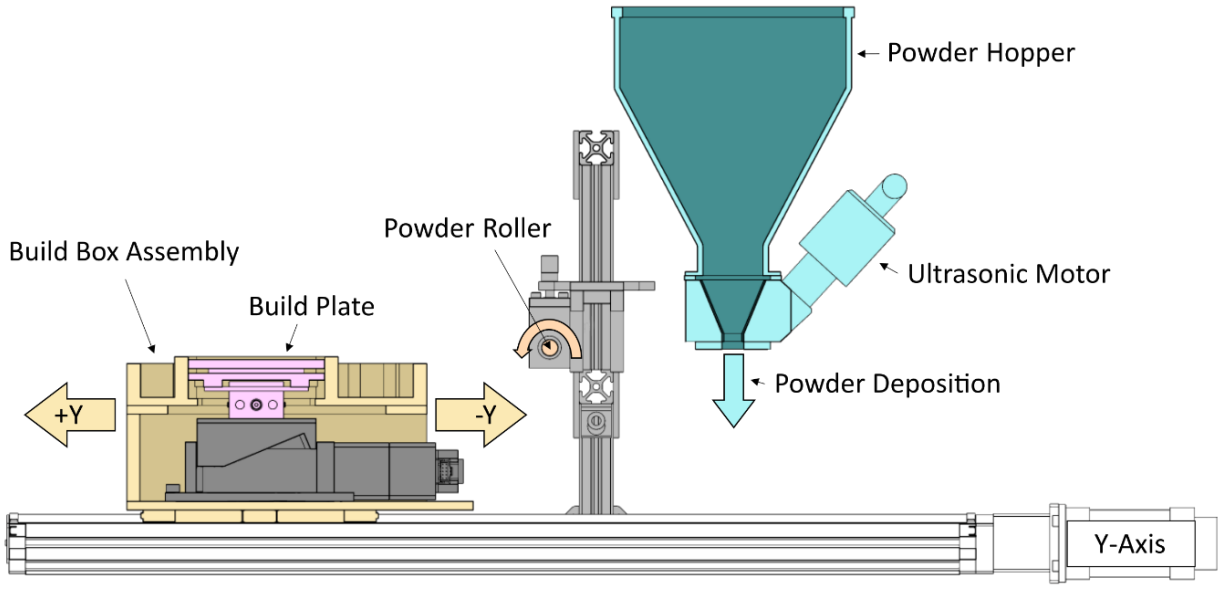

Figure 7. Cross section view of powder and deposition system. The build box assembly traverses along the Y-axis to position the build box under the hopper and roller for powder deposition and spreading. When rolling a new layer, the build box first moves to the far right in the image and then travels left under the hopper and roller to receive powder and roll the new layer.

Removable Build Box

The printer features a removable build box with a reservoir for excess powder surrounding the build platform. The build box can be removed for part curing and extraction, as well as for removing excess powder after prints for recycling. The build box is attached to the Y-axis using four bolts and the build platform is connected to Z-axis using a manually actuated gripper mechanism. The gripper was designed to ensure that the build platform is aligned properly with both the Z-axis and build box to avoid binding during motion. The gripper can be actuated to connect or disconnect the build platform using two fine adjustment screws visible through openings on both sides of the build box assembly.

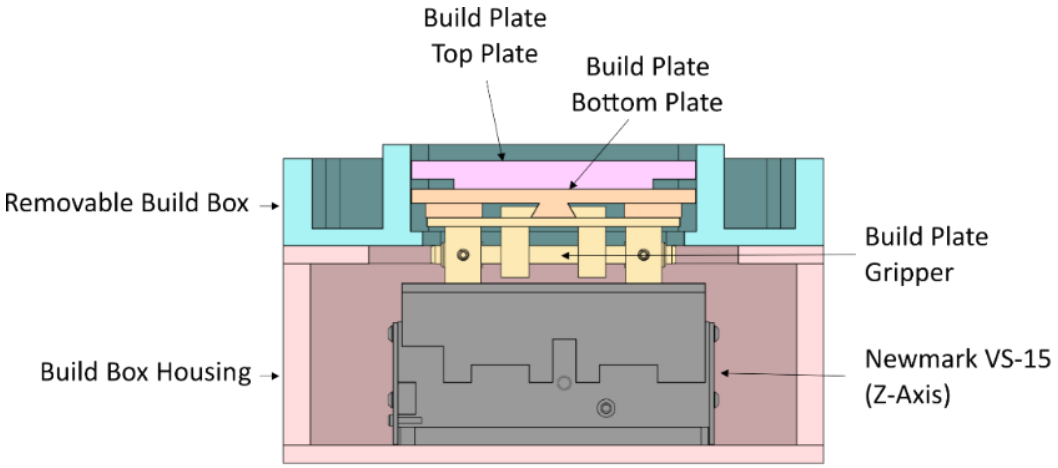

Figure 8. Cross section view of the build box assembly. The build plate is made of a top and bottom plate to accommodate a felt seal that prevents powder from escaping between the build plate and build box. The build plate is mounted to the Z-axis using a manually actuated gripper.

High-Speed X-Ray Imaging Compatibility

The compact design and open format of the custom BJ system enables integration with other equipment for specialized testing. The build box assembly can be removed and replaced for testing that requires a different build box size or configuration. A custom sample holder mount that attaches to the Y-axis was designed to enable observation of the printing process with high-speed synchrotron X-rays at the Advanced Photon Source in the Argonne National Laboratory. The imaging setup used at the Advanced Photon Source is described in detail by Parab, et al [14].

The open design of the printer enabled the X-ray source to pass through the sample during printing without obstruction from other components, and the custom sample holder mount allowed printing in a powder bed thin enough for X-ray transmission. The printer is equipped with a digital output connecter that can be used to trigger external measurement equipment at a user-specified time before the printhead reaches a desired position during printing. This output trigger was used to synchronize printer operation, high-speed X-ray capture, and optical high-speed image capture during testing at the Advanced Photon Source [19].

Control Software

The printer is controlled by custom desktop software that handles communications with the Galil motion controller, JetDrive controller, and droplet observation USB camera. All software is available at [17]. The software includes functionality for manual operation of printer motion stages and modules. A user interface is provided for printing primitives which allows the user to set key printing parameters for desired testing. Once testing parameters have been selected by the user and the user selects to start the print, the software sends commands over ethernet to the Galil motion controller which the controller then processes into signals sent to the motion stages to achieve desired movement. Direct communication with the JetDrive controller over RS-232 is integrated into the software and allows for jetting parameters to be automatically changed during or between prints. The software incorporates an SDK provided by the manufacturer for the USB camera to enable integrated observation of camera footage and control over imaging parameters used for droplet observation. The user interface for observing droplets and setting imaging and jetting parameters is shown in Figure 9.

The desktop software was developed in C++ using the Qt5 framework. Communication with the Galil motion controller is handled by the Galil gclib API. Communication with the USB camera is handled by the IDS ueye SDK [17].

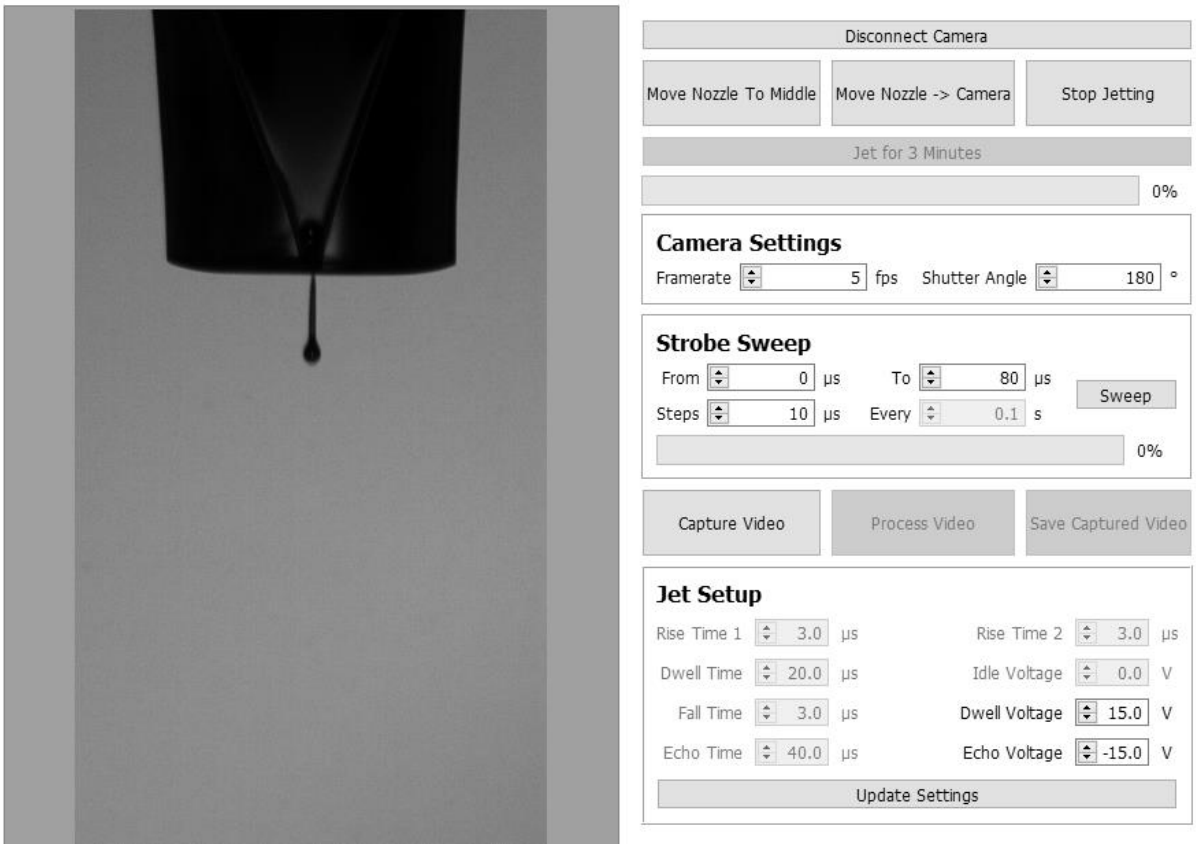

Figure 9. Screenshot of the custom PC host software used to control the BJ printer. The user interface shown is used for observing droplet formation using the droplet observation camera and setting jetting parameters for use during printing.

System Validation

Powder Deposition and Spreading

Powder deposition and spreading performance of the custom BJ system was measured by preparing a rolled powder bed of stainless steel 316L powder and measuring the packing fraction of the powder bed. The stainless steel 316L powder used had a volume average particle diameter (Dv50) of 10.0 µm (Dv10 of 3.92 µm and Dv90 of 22.0 µm)[15]. The powder bed spread density was measured by rolling a powder bed with 100 layers and using a sharp cylindrical punch with a known inner diameter to isolate a known volume of powder [6]. Powder external to the punch was brushed away and the powder inside the punch was weighed to calculate the powder bed spread density. The packing fraction of the powder bed prepared on the custom BJ system was calculated as 55%, indicating that the powder deposition and spreading capabilities of the printer are sufficient to produce parts that can be effectively densified during sintering [1].

Printhead Accuracy

To evaluate the performance of the inkjet printing capabilities of the custom BJ printer, a grid of dyed binder droplets was printed on photopaper, and individual measured droplet positions were compared to the commanded positions. The grid was printed with a droplet spacing of 250 µm between each droplet and 20 droplets were printed in each direction to form a 5 mm square grid of droplets. Figure 10 shows an image taken on a Keyence VHX-7000 microscope of a printed grid. During testing, the printer starts in the bottom left of the image and scans across each row from left to right to print the grid. The printhead returns to the left side of the grid before each row is printed so each row is printed left to right. The microscope image shown in Figure 10 was processed in ImageJ (FIJI) to calculate the position of the center of each droplet. The grid of measured droplet positions was then aligned to the grid of commanded droplet positions to measure the placement error of individual droplets. Absolute error in both the X and Y directions was calculated for each droplet by calculating the difference in position between the droplet in the regular commanded grid and the measured position of the droplet after printing. Error in the X and Y directions was combined to produce Figure 11 which depicts each measured droplet superimposed over the commanded droplet position where measured droplets are color-coded by the total absolute positional error of the droplet.

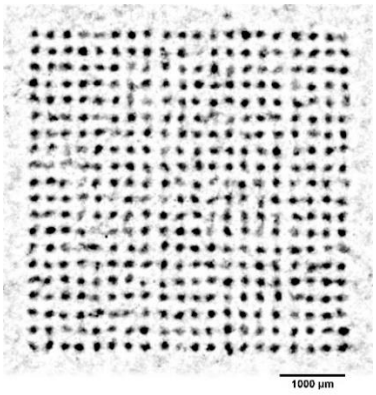

Figure 10. Microscope image of a printed grid of droplets on photopaper. Images were taken on the Keyence VHX-7000 Microscope. The print was conducted with a droplet spacing of 250 µm.

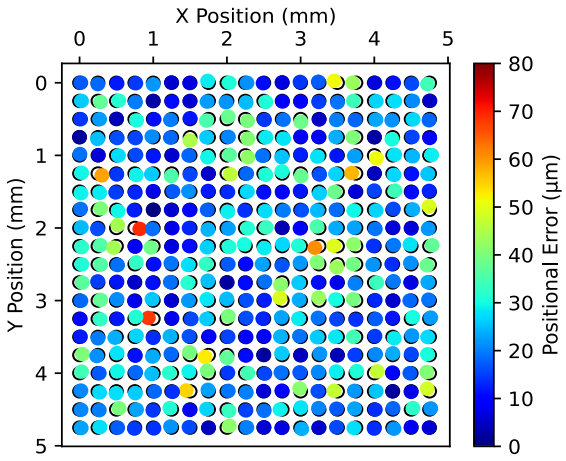

Figure 11. Color-map of droplet positional error in a printed grid. Colored circles show measured positions of printed droplets which are graphed over black outlines of the commanded droplet positions.

When aligning the printed grid with the grid of commanded droplet positions for analysis, an iterative closet point (ICP) least squares regression optimization method was implemented. This alignment minimized the total error between all droplets and was used to produce the result shown in Figure 11. The average and standard deviation in absolute error for this test of the X (nozzle movement direction) and Y-axis is 16.3 ± 12 µm and 11.9 ± 9.5 µm respectively.

Conclusions

This custom laboratory-scale BJ system was constructed to better understand the BJ process. Capable of powder deposition, powder rolling, compatibility with many powder types and sizes, and control over layer thickness allow the powder bed to be customized for studying the BJ process. The high-accuracy motion system enables consistent printing performance for demanding printing conditions. The modular approach of the printer design allows for capabilities to be added for tests that require additional components. Finally, a droplet observation camera provides the capability to observe and measure jetting parameters which enables insight into effects of droplet velocity and volume on the BJ process. Additional features to be added in the future for greater functionality include a heat lamp and a second roller. The current printer and future modules will enable a growing range of experiments the custom BJ system will perform to better understand the BJ process.

Acknowledgments

This material is based upon work supported by the National Science Foundation through award number CMMI-1946724 and NRC 31310019M0006.

Disclaimer: Any opinions, findings, and conclusions or recommendations expressed in this material are those of the author(s) and do not necessarily reflect the views of the National Science Foundation.

References

[1] M. Ziaee, N.B. Crane, Binder jetting: A review of process, materials, and methods, Additive Manufacturing, 28 (2019) 781-801.

[2] M. Li, W. Du, A. Elwany, Z. Pei, C. Ma, Metal Binder Jetting Additive Manufacturing: A Literature Review, Journal of Manufacturing Science and Engineering, 142 (2020) 1-45.

[3] I.a. Gibson, D.a. Rosen, B.a. Stucker, Additive manufacturing technologies : 3D printing, rapid prototyping, and direct digital manufacturing, Second edition. ed., Springer, New York, NY, 2015.

[4] E. Sachs, M. Cima, P. Williams, D. Brancazio, J. Cornie, Three dimensional printing. Rapid Tooling and prototypes directly from a CAD model, Journal of engineering for industry, 114 (1992) 481-488.

[5] Y. Bai, C.B. Williams, An exploration of binder jetting of copper, Rapid Prototyping Journal, 21 (2015) 177-185.

[6] M. Ziaee, E.M. Tridas, N.B. Crane, Binder-Jet Printing of Fine Stainless Steel Powder with Varied Final Density, Jom, 69 (2016) 592-596.

[7] T. Sivarupan, N. Balasubramani, P. Saxena, D. Nagarajan, M. El Mansori, K. Salonitis, M. Jolly, M.S. Dargusch, A review on the progress and challenges of binder jet 3D printing of sand moulds for advanced casting, Additive Manufacturing, 40 (2021).

[8] X. Lv, F. Ye, L. Cheng, S. Fan, Y. Liu, Binder jetting of ceramics: Powders, binders, printing parameters, equipment, and post-treatment, Ceramics International, 45 (2019) 12609-12624.

[9] T. Colton, J. Liechty, A. McLean, N. Crane, Influence of drop velocity and droplet spacing on the equilibrium saturation level in binder jetting, in: 30th Annual International Solid Freeform Fabrication Symposium - An Additive Manufacturing Conference, SFF 2019, August 12, 2019 - August 14, 2019, The University of Texas at Austin, Austin, TX, United states, 2019, pp. 99-108.

[10] T. Colton, C. Inkley, A. Berry, N.B. Crane, Impact of inkjet printing parameters and environmental conditions on formation of 2D and 3D binder jetting geometries, Journal of Manufacturing Processes, 71 (2021) 187-196.

[11] T. Fan, Droplet-Powder Impact Interaction In Three Dimensional Printing, in, Massachusetts Institute Of Technology, 1995.

[12] B. Barthel, F. Janas, S. Wieland, Powder condition and spreading parameter impact on green and sintered density in metal binder jetting, Powder Metallurgy, 64 (2021) 378-386.

[13] Y. Bai, G. Wagner, C.B. Williams, Effect of Particle Size Distribution on Powder Packing and Sintering in Binder Jetting Additive Manufacturing of Metals, Journal of Manufacturing Science and Engineering, 139 (2017).

[14] N.D. Parab, J.E. Barnes, C. Zhao, R.W. Cunningham, K. Fezzaa, A.D. Rollett, T. Sun, Real time observation of binder jetting printing process using high-speed X-ray imaging, Scientific Reports, 9 (2019) 2499.

[15] T. Colton, N.B. Crane, Influence of droplet velocity, spacing, and inter-arrival time on line formation and saturation in binder jet additive manufacturing, Additive Manufacturing, 37 (2021).

[16] D. Oropeza, A.J. Hart, A laboratory-scale binder jet additive manufacturing testbed for process exploration and material development, Int J Adv Manuf Technol, 114 (2021) 3459-3473.

[17] J. Lawrence, GitHub: BYUCreateLab/CREATE_Lab_BJ_Printer, https://github.com/BYUCreateLab/CREATE_Lab_BJ_Printer.git, in, 2022.

[18] A. van der Bos, M.-J. van der Meulen, T. Driessen, M. van den Berg, H. Reinten, H. Wijshoff, M. Versluis, D. Lohse, Velocity Profile inside Piezoacoustic Inkjet Droplets in Flight: Comparison between Experiment and Numerical Simulation, Physical Review Applied, 1 (2014) 014004.

[19] J. Lawrence, C. Inkley, K. Fezzaa, S.J. Clark, N.B. Crane, Observation of Binder Jetting Defect Formation Using High-Speed Synchrotron X-Ray Imaging, in: Solid Freeform Fabrication Symposium An Additive Manufacturing Conference Austin, TX, USA, 2022.